

Graph Elimination Networks

Shuo Wang

202121632843@smail.xtu.edu.cn

Xiangtan University

Xiangtan, China

Ge Cheng

chengge@xtu.edu.cn

Xiangtan University

Xiangtan, China

Yun Zhang

yunzhangcn@outlook.com

Hunan University

Hunan, China

ABSTRACT

Graph Neural Networks (GNNs) are widely applied across various domains, yet they perform poorly in deep layers. Existing research typically attributes this problem to node over-smoothing, where node representations become indistinguishable after multiple rounds of propagation. In this paper, we delve into the neighborhood propagation mechanism of GNNs and discover that the real root cause of GNNs' performance degradation in deep layers lies in ineffective neighborhood feature propagation. This propagation leads to an exponential growth of a node's current representation at every propagation step, making it extremely challenging to capture valuable dependencies between long-distance nodes. To address this issue, we introduce Graph Elimination Networks (GENs), which employ a specific algorithm to eliminate redundancies during neighborhood propagation. We demonstrate that GENs can enhance nodes' perception of distant neighborhoods and extend the depth of network propagation. Extensive experiments show that GENs outperform the state-of-the-art methods on various graph-level and node-level datasets.

CCS CONCEPTS

• **Computing methodologies** → Artificial intelligence; *Neural networks*; • **Theory of computation** → *Graph algorithms analysis*.

KEYWORDS

Graph Neural Network, Deep Graph Neural Network, Graph Self-Attention, Subgraph Self-Attention, Algorithm Framework

1 INTRODUCTION

Graph neural networks (GNNs) [31] are a powerful method for handling non-Euclidean data, and have demonstrated remarkable potential in various domains, such as social networks [1], recommendation systems [7], bioinformatics [16, 20, 38], chemistry [6, 33], and physics [26]. The mainstream algorithms in GNNs, such as GCN [15], GAT [30], SAGE [12], etc., recursively update node representations using direct neighbors, and stack multiple layers to enlarge the receptive field [10]. Despite their outstanding performance in various graph-related tasks, previous studies [11, 14, 39] have revealed that the performance of mainstream GNNs deteriorates significantly when the number of stacked layers is large, which restricts their potential and applicability.

This problem has been attributed to node over-smoothing by previous studies [2, 19, 23, 37], that is, deep propagation causes different node representations to become indistinguishable. However, recent research [21, 36] indicates that the curve measuring the degree of node representation smoothness deviates significantly from the actual model outcome curve. In shallow GNNs, the network performance can still decline even if the node representations

are not sufficiently smooth. In recent years, some attempts have been made to extend mainstream GNNs to deeper layers [8, 24]. The first type of methods, such as DeeperGNN [17, 18] and GCNII [5], etc., ensure that no matter how many layers the GNN passes, the initial features will not be overwritten during the update by using initial residuals, identity mapping, dense connections, and replacing aggregation functions. This indeed greatly enhances the model's ability to distinguish graph spatial structure features, but it doesn't change the fact that feature transfer between two distant nodes remains extremely challenging. The second type of methods, such as DAGNN [21], etc., use decoupling operations [4, 9, 28] to break the symmetry of propagation and update, enabling GNNs to propagate to farther places at a very low cost. However, these methods cannot avoid the redundancy in the propagation process, and their performance peaks are still concentrated in the shallow layers, with limited improvement compared to mainstream GNNs. Our study shows that when using direct neighbors to recursively update node representations, as the number of recursions increases, the current node representations will experience exponential redundant growth, while the features propagated from afar through direct neighbors will always be 1. Therefore, even if the model can propagate deeper hops, it offers minimal assistance in capturing long-distance dependencies between two nodes. We believe that this problem severely limits the performance of mainstream GNNs when stacking multiple layers. Taking GCN as an example, assuming there are two nodes 4 hops apart, after 4 layers of GCN transmission, when the right node feature is transmitted to the left, its norm will retain at most 1.85% of the original feature. This indicates that no matter how large the initial difference between the two nodes is, 4-layer GCN will have difficulty learning this difference.

To address the above problem, we propose a new method, namely Graph Elimination Networks (GENs). GENs reduce redundancy in propagation by performing elimination calculations during propagation. Moreover, it also pays attention to the network's ability to extract node representations itself. By calculating self-attention within the K-hop receptive field subgraph of each node, it approximates the effect of using Transformer on each subgraph [3, 29, 34], and its cost is usually much lower. We theoretically show that GENs preserve the mainstream GNN's ability to extract structural features while supporting self-attention calculation within each node's K-hop receptive field subgraph. It is not only suitable for deeper propagation but also has stronger expressive power. Finally, our experimental results on graph-level and node-level tasks from different domains including OGB datasets [13] prove that our proposed graph elimination networks achieves significantly better performance than existing GNN methods. Our contributions are as follows:

- We reveal the critical defect of neighborhood propagation methods that causes node representations to undergo exponential growth in propagation, resulting in redundancy that severely impairs the performance of GNNs in deep propagation.
- We propose graph elimination networks, which mitigate the redundancy problem in neighborhood propagation, and exhibit stronger expressive power than mainstream GNNs.
- We perform extensive experimental evaluations on graph-level and node-level tasks from different domains, and demonstrate the superiority of our proposed algorithm.

2 PRELIMINARIES

2.1 Message Passing Neural Network

Message Passing Neural Network (MPNN) [10] is a general framework for GNNs models that encompasses various specific models such as GCN, GAT, and GIN [32]. The MPNN framework consists of two phases, Message Passing and Readout. The Message Passing phase can be further divided into two steps: Neighborhood Propagation and Update. Generally, the node representations are updated at the l -th layer according to the following formula:

$$\begin{aligned} a_i^{(l)} &= \text{Propagation}^{(l)} \left(\left\{ h_i^{(l-1)}, \left\{ h_j^{(l-1)} \mid j \in \mu(i) \right\} \right\} \right) \\ h_i^{(l)} &= \text{Update}^{(l)} \left(a_i^{(l)} \right), \end{aligned} \quad (1)$$

where $h_i^{(l)} \in R^n$ is the feature representation of node i at layer l and $\mu(i)$ is the set of neighbor nodes of i . Models based on the MPNN framework are simple and efficient to implement. However, when the number of layers exceeds 3 or 4, their accuracy gradually decreases, which limits their ability to perform depth propagation.

2.2 Redundancy in Neighborhood Propagation

We noticed that models following the MPNN framework conduct multiple neighborhood propagation steps. This leads to the representation of each node being continuously returned through its neighbors, causing an exponential growth of the node's own representation and the representations of its neighbors. To demonstrate this problem, we use GCN as an example. Because GCN adheres to the MPNN framework, the notation below differs from the original paper, but the outcome is equivalent. its formula can be written as:

$$h_i^{(l)} = f \left(W_l \left(C_{ii} h_i^{(l-1)} + \sum_{j \in \mu(i)-i} C_{ij} h_j^{(l-1)} \right) \right), \quad (2)$$

where $f(\cdot)$ is the nonlinear function between layers, such as the composite function $\text{Relu}(\text{BN}(\cdot))$ that consists of the activation function Relu and Batch Normalization. W_l is the learnable parameter matrix for the l -th layer, C_{ij} is used to normalize the node representations, such that $C_{ij} = d_i^{-1/2} * d_j^{-1/2}$, and d_i denotes the degree of node i . Figure 1 illustrates the propagation of node features in message passing.

Without the normalization coefficient C_{ij} , the number of initial features in the aggregated result of node A grows exponentially, and the specific number of the first 10 hops is as follows: 1, 3, 7, 18, 46, 120, 316, 840, 2248 and 6048. Even though in GCNs the normalization coefficient C_{ij} ensures that the norm of node representations

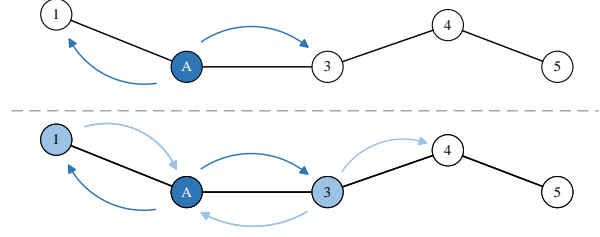


Figure 1: The schematic diagram of feature propagation in message passing, where the feature of node A is passed to its neighbor nodes in 1-hop, and then passed back to itself in 2-hop through the neighbors.

does not change drastically, it is unable to slow down this intensifying trend. According to Eq.(2), when the representation of node 5 propagates to the representation of node 1 through 4 hops, it needs to be multiplied by $-1/\sqrt{6}, 1/3, 1/3, -1/\sqrt{6}$ consecutively, and the norm of it when it reaches node 1 is only up to 1.85% of the original norm of the feature of node 5. We introduce this phenomenon as 'redundancy in neighborhood propagation', which makes it extremely challenging for GNNs to capture long-distance dependencies between two nodes. This explains why mainstream GNNs usually degrade after stacking more layers. The experimental results shown in Figure 5 indicate that, without taking additional measures to mitigate excessive node smoothness, GNNs significantly expand the model's propagation depth simply by limiting redundancy in propagation.

3 GRAPH ELIMINATION ALGORITHM

In this section, we introduce an algorithm to address redundancy during neighborhood propagation, outlined in the propagation phase of Figure 2. The goal is to eliminate already-included features from the current node during each propagation. We'll demonstrate this using the GCN for formula derivation, but the method applies to other mainstream GNNs. It's evident that there's no redundancy in the first propagation of the GCN, so we directly consider the process of the second propagation, as described by Eq.(2):

$$h_i^{(2)} = f \left(W_2 \left(C_{ii} h_i^{(1)} + \sum_{j \in \mu(i)-i} C_{ij} h_j^{(1)} \right) \right). \quad (3)$$

Since f and W almost always occur together, we simplify the notation by omitting the parentheses between f and W in the following equations. By rearranging the second term on the right-hand side of the equation, we obtain:

$$\begin{aligned} \sum_{j \in \mu(i)-i} C_{ij} h_j^{(1)} &= \sum_{j \in \mu(i)-i} C_{ij} f W_1 \left(C_{jj} h_j^{(0)} \right) \\ &\quad + C_{ji} h_i^{(0)} + \sum_{k \in \mu(j)-j-i} C_{jk} h_k^{(0)}. \end{aligned} \quad (4)$$

Given that $f(\cdot)$ is a nonlinear function, we usually cannot simplify this equation further. However, for the sake of discussion, we assume that $f(\cdot)$ is $\text{Relu} = \max(0, x)$, and that all the initial features $h^{(0)}$ have the same sign and all the parameters in the same

column of W have the same sign as well. Under these assumptions, we can split the terms inside the nonlinear function. Note that C_{ij} is always non-negative, so we have:

$$\begin{aligned} \sum_{j \in \mu(i)-i} C_{ij} h_j^{(1)} &= \sum_{j \in \mu(i)-i} C_{ij} W_1 \sum_{k \in \mu(j)-j-i} C_{jk} h_k^{(0)} \\ &+ \sum_{j \in \mu(i)-i} C_{ij} \left| W_1 \sum_{k \in \mu(j)-j-i} C_{jk} h_k^{(0)} \right| \\ &+ \sum_{j \in \mu(i)-i} C_{ij} W_1 \left(C_{jj} h_j^{(0)} + C_{ji} h_i^{(0)} \right) \\ &+ \sum_{j \in \mu(i)-i} C_{ij} \left(\left| W_1 \left(C_{jj} h_j^{(0)} + C_{ji} h_i^{(0)} \right) \right| \right), \end{aligned} \quad (5)$$

there $h_i^{(1)}$ already contains the features of the adjacent hop, we consider the features in this equation that correspond to the 0-hop and the 1-hop to be redundant, i.e., we need to remove the 3rd and 4th terms from the right-hand side of the equation. We denote the removed term as:

$$del_1 = \sum_{j \in \mu(i)-i} C_{ij} f W_1 \left(C_{jj} h_j^{(0)} + C_{ji} h_i^{(0)} \right). \quad (6)$$

After eliminating the redundant expression of features, $h_i^{(2)}$ can be written as:

$$h_i^{(2)} = f W_2 \left(C_{ii} h_i^{(1)} - del_1 + \sum_{j \in \mu(i)-i} C_{ij} h_j^{(1)} \right). \quad (7)$$

Moreover, based on Eq.(5), we can derive another form of this equation:

$$h_i^{(2)} = f W_2 \left(C_{ii} h_i^{(1)} + \sum_{j \in \mu(i)-i} C_{ij} f W_1 \sum_{k \in \mu(j)-j-i} C_{jk} h_k^{(0)} \right). \quad (8)$$

Eq.(8) reveals that the elimination process removes all the existing features that are propagated from the neighborhood, thus keeping only the new features. We can further derive a nested function as follows, see Appendix A.1 for the detailed derivation:

$$\begin{aligned} f_1^E &= C_{ij} f W_1 \left(C_{jj} h_j^{(0)} + C_{ji} h_i^{(0)} \right), \\ f_2^E &= C_{ij} f W_2 \left(C_{jj} h_j^{(1)} + C_{ji} h_i^{(1)} - C_{ji} f W_1 \left(C_{ii} h_i^{(0)} + C_{ij} h_j^{(0)} \right) \right), \\ &\dots \\ f_l^E &= C_{ij} f W_l \left(C_{jj} h_j^{(l-1)} + C_{ji} h_i^{(l-1)} - C_{ji} f W_{l-1} \left(C_{ii} h_i^{(l-2)} \right. \right. \\ &\quad \left. \left. + C_{ij} h_j^{(l-2)} - f W_{l-2} f_{l-2}^E \right) \right), \end{aligned} \quad (9)$$

where $l \geq 2$, E is short for Elimination and $f_0^E = 0$. The removed term of the $l+1$ layer can then be written as:

$$del_l = \sum_{j \in \mu(i)-i} f_l^E. \quad (10)$$

In the algorithmic implementation, Eq.(10) can be recast as follows. Clearly, the complexity of the elimination is determined by the number of edges in the graph, aligning with $O(|\mathcal{E}|)$, which is consistent with the methodology of the MPNN framework.

$$\begin{aligned} del_l &= C_{ji}^{(l+1)} f W_l \left(C_{ii}^{(l)} h_i^{(l-1)} + C_{ij}^{(l)} h_j^{(l-1)} - dl_{l-1} \right), \\ dl_l &= C_{ij}^{(l+1)} f W_l \left(C_{jj}^{(l)} h_j^{(l-1)} + C_{ji}^{(l)} h_i^{(l-1)} - del_{l-1} \right), \\ del_l &= \sum_{j \in \mu(i)-i} dl_l, \end{aligned} \quad (11)$$

where $del_0 = dl_0 = 0$, $C_{ij}^{(l)}$ is the propagation coefficient from node j to node i in the l -th layer. The formula for the $l+1$ layer of the GCN after eliminating the redundant of features is:

$$h_i^{(l+1)} = f W_{l+1} \left(C_{ii} h_i^{(l)} - del_l + \sum_{j \in \mu(i)-i} C_{ij} h_j^{(l)} \right). \quad (12)$$

We call the aforementioned calculation method as the 'graph elimination algorithm', which has been validated experimentally. It's crucial to emphasize that this algorithm comes with strict preconditions. Given that we cannot ascertain the presence of cycles in distant nodes based solely on 1-hop neighborhood information, we must assume all graphs are acyclic. Consequently, the algorithm is solely suited for acyclic graphs.

4 METHODOLOGY

In this section, we present our proposed graph elimination networks in detail and explain how to apply the graph elimination algorithm to our neural network. Similar to mainstream GNNs, the graph elimination networks follows the MPNN framework, so we explain it in two parts, neighborhood propagation and update, separately. At the end of this section, we also provide a theoretical analysis of the performance of GENs.

4.1 Neighborhood Propagation

Directly applying the graph elimination algorithm to GNNs is infeasible and futile due to the stringent constraints. The graph elimination algorithm flattens all the nodes within a node's receptive field, which impairs the node's ability to distinguish the spatial structure information of its neighborhood. This adversely affects the performance of GNNs. Thus, we opt for limiting the redundancy in neighborhood propagation. This also enables us to avoid the cumbersome nonlinear functions and focus on elimination in a single-layer network. Although the graph elimination algorithm is not applicable to cyclic graphs, which leads to the algorithm's inability to handle the redundancy caused by cycles. However, our experimental results show that GENs still perform well on most real-world datasets.

Figure 2 illustrates our model, which has a decoupled structure. This means that it can perform multiple rounds of propagation without computing any learnable parameters in the neighborhood propagation phase. Decoupling yields two benefits: 1) it removes the strict restriction of the model depth on the expansion of the receptive field, so that the node's sensory range is no longer limited by the model degradation problem [36] caused by increasing the model depth; and 2) it circumvents the restriction of the nonlinear operation between layers, which ensures that the premise assumptions of the elimination algorithm are met.

Next, we denote the output of the GENs at the L -th layer as X^L , and use the symbol $h^{(L,k)}$ to represent the result of the k -th propagation in the GENs at the L -th layer. We will show the calculation process in the L -th layer of the GENs in the following text. For simplicity, and under the premise that it will not cause ambiguity, we will abbreviate $h^{(L,k)}$ as $h^{(k)}$, and the same for other symbols.

Specifically, we compute the removed item in the k -th propagation after decoupling as follows:

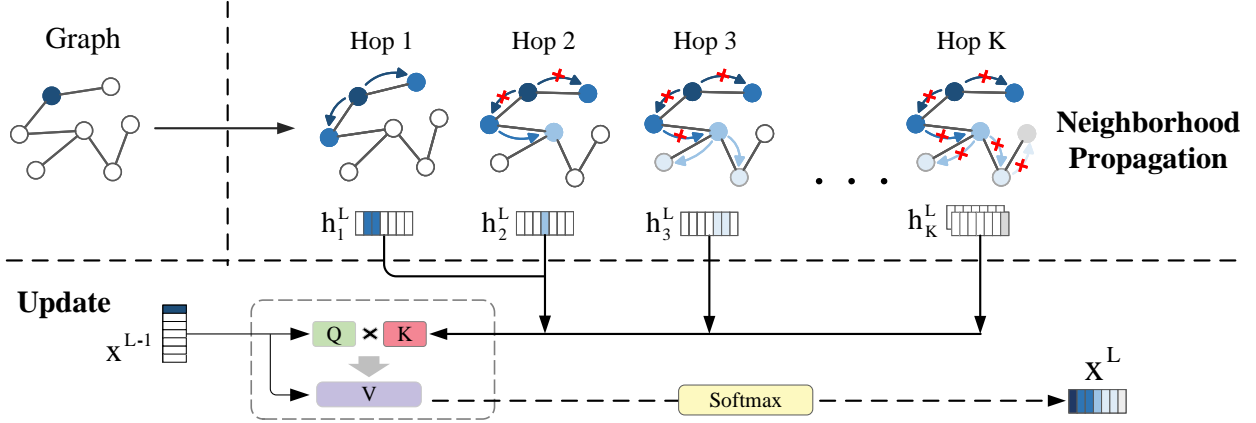


Figure 2: A schematic diagram of the graph elimination networks in the L -th layer. The network has two phases: neighborhood propagation and update. In propagation, node features undergo K rounds of propagation, with the elimination algorithm applied each round to distinguish and obtain features of neighbors at different hops. During the update, self-attention is computed between the node and its K -hop neighbors, followed by feature extraction from a linear layer for a new node representation. Initial features are represented using a one-hot embedding.

$$\begin{aligned}
 de_{k-1} &= C_{ji}^{(k)} \left(C_{ii}^{(k-1)} h_i^{(k-2)} + C_{ij}^{(k-1)} h_j^{(k-2)} - dl_{k-2} \right), \\
 dl_{k-1} &= C_{ij}^{(k)} \left(C_{jj}^{(k-1)} h_j^{(k-2)} + C_{ji}^{(k-1)} h_i^{(k-2)} - de_{k-2} \right), \\
 del_{k-1} &= \sum_{j \in \mu(i)-i} dl_{k-1}, \quad (13)
 \end{aligned}$$

where $dl_0 = 0$, $de_0 = 0$, and $C_{ij}^{(k)}$ is the propagation coefficient of the k -th time, which depends on the different propagation modes, and it is usually $C_{ij}^{(k)} \neq C_{ji}^{(k)}$. Finally, the output of the propagation of GENs is given by the following equation:

$$h_i^{(k)} = C_{ii}^{(k)} h_i^{(k-1)} - del_{k-1} + \sum_{j \in \mu(i)-i} C_{ij}^{(k)} h_j^{(k-1)}. \quad (14)$$

Referring to Eq.(8), after removing $C_{ii}^{(k)} h_i^{(k-1)}$, we obtain the valuable features of the nodes that are only k hops away from the node in the receptive field. After repeating the propagation K times, we concatenate all the results with the initial features to form a matrix and output it. The matrix is denoted as:

$$\hat{H}_i = \text{concat} \left(h_i^{(0)}, h_i^{(1)}, h_i^{(2)}, \dots, h_i^{(K)} \right) \in R^{(K+1) \times n}, \quad (15)$$

where $\text{concat}(\cdot)$ is used to stack vectors into matrices.

4.2 Update

To update the initial node representations, we use the partitioned K -hop node features obtained from the propagation process. Our aim is to enhance the node's ability to capture the boundaries of its receptive field, so we adopt a simple and efficient update method

that sums up the $K+1$ feature vectors in \hat{H}_i . Then, we apply a linear layer to learn the features of the node's neighborhood, another linear layer to learn the features of the node itself, and add them together as the output of the GENs layer. The update method of the GENs in the L -th layer is expressed by the following equation:

$$X_i^L = h_i^{(0)} W_1^L + \sum_{k=0}^K h_i^{(k)} W_2^L, \quad (16)$$

where W_1^L and W_2^L are two distinct learnable parameters.

As shown in Eq.(15), we obtain the matrix \hat{H} after the propagation process. We can then use a simple self-attention computation to avoid relying on the neighborhood path features for GAT propagation. We explain the problem with GAT as follows: on an acyclic graph, for any node x_{ik} that is in the receptive field of node x_i , there is a path $x_i x_{i1} x_{i2} \dots x_{ik}$ that connects x_i and x_{ik} . The ratio of features that are propagated from all the nodes along this path to x_i is always higher than or equal to that of x_{ik} . We introduce another update method for GENs that integrates the K -hop self-attention with the self-attention propagation of GAT. This method employs two separate self-attention vectors to capture the self-attention of each node in its receptive field. We first present the decoupled self-attention propagation formula as:

$$\begin{aligned}
 e_{ij} &= \text{LeakReLU} \left(a^T \left[h_i^{(k-1)} || h_j^{(k-1)} \right] \right), \\
 \alpha_{ij} &= \text{softmax} \left(e_{ij} \right), \\
 h_i^{(k)} &= -del_{k-1} + \sum_{j \in \mu(i)} \alpha_{ij} h_j^{(k-1)}, \quad (17)
 \end{aligned}$$

where $a^T \in R^{2 \times n}$ is a learnable parameter for computing the edge self-attention, which is constant in the multiple propagation process, and del_{k-1} is obtained from Eq.(13). The update method of

$$\begin{pmatrix} \alpha_{ii} * \beta_{h0} & 0 & 0 & 0 & 0 & 0 \\ 0 & \alpha_{ij_1} * \beta_{h1} & 0 & 0 & 0 & 0 \\ 0 & \alpha_{ij_2} * \beta_{h1} & 0 & 0 & 0 & 0 \\ 0 & 0 & \alpha_{ij_2} * \alpha_{jk_1} * \beta_{h2} & 0 & 0 & 0 \\ 0 & 0 & 0 & \alpha_{ij_2} * \alpha_{jk_1} * \alpha_{kl_1} * \beta_{h3} & 0 & 0 \\ 0 & 0 & 0 & \alpha_{ij_2} * \alpha_{jk_1} * \alpha_{kl_2} * \beta_{h3} & 0 & 0 \\ 0 & 0 & 0 & 0 & \alpha_{ij_2} * \alpha_{jk_1} * \alpha_{kl_1} * \alpha_{lm_1} * \beta_{h4} & 0 \end{pmatrix}$$

Figure 3: The matrix of feature compositions for the blue node on the acyclic graph from Figure 2, with $K=4$ in GENs (SubG). Each row corresponds to a node on the graph, and each column corresponds to a different hop distance from the blue node, starting from zero. By employing two distinct self-attention coefficients, α and β , GENs (SubG) can adaptively access the features of any node within its receptive field.

node neighborhood representations can then be expressed as:

$$\begin{aligned} \beta_i &= h_i^{(0)} W_q^L (\hat{H}_i W_k^L)^T, \\ X_i^L &= h_i^{(0)} W_1^L + \text{softmax}(\beta_i) \hat{H}_i W_2^L, \end{aligned} \quad (18)$$

where \hat{H} is obtained from Eq.(15), W_q^L and W_k^L are the learnable parameters for the K -hop self-attention, and X_i^L is the output result after updating. We refer to the GENs with this update method as GENs (SubG).

4.3 Performance Analysis

In this section, we analyze the performance of GENs. Figure 3 displays the composition of a node’s output representation vector when $K=4$. Coefficients above the diagonal were originally present but were set to zero after eliminating redundancies. There are two update methods mentioned earlier. For Eq.(16), it is equivalent to applying the elimination algorithm directly to mainstream GNNs like GCN and GAT. In this context, it corresponds to the matrix form where the second-term self-attention coefficient β is set to 1. At this time, GENs enhance the model’s ability to capture long-distance node dependencies by reducing redundancy growth, and when α is less than 1, it retains the trend that closer features are more important. However, a potential drawback is the loss of some degree-related information, as the node degree determines the speed of redundancy growth in the node representations, which GENs eliminate. Nonetheless, experimental results indicate that the benefits of enhanced capability in capturing long-distance node dependencies outweigh this limitation.

As discussed in the previous section, relying solely on α leads to the problem of dependency on neighborhood path features. GEN (SubG) addresses this issue by utilizing K -hop self-attention, which is when adopting Eq.(18). For instance, if we want to obtain the feature of the fifth node on the matrix, we can set $\alpha_{i,j_2} * \alpha_{j_2,k_1} * \alpha_{k_1,l_1} = 1$ and $\beta_{h3} = 1$. Then we have $A_{6,4}^{(i)} = 1$ and all other entries of $A^{(i)}$ are 0. According to Eq.(18), we obtain $X_i^L = h_i^{(L,0)} W_1^L + h_{l_1}^{(L,0)} W_2^L$. This demonstrates that GENs (SubG) can adaptively access the features of any node in the receptive field like Transformer. For graphs with cycles, the situation becomes more complex. However, as depicted in Figure 4, any such graph can be represented as an acyclic graph within a shadow space, augmented with additional shadow nodes. From the initial node’s perspective, this acyclic representation and

the original cyclic graph are equivalent. Based on our discussions, GEN (SubG) retains the ability to adaptively access any node within this acyclic representation. However, the presence of cycles can cause some graphs to be interpreted as infinitely expansive acyclic graphs, potentially leading to different cyclic graphs being perceived as the same. It’s important to emphasize that this challenge is not unique to our method but is a general limitation among techniques utilizing neighborhood propagation. In summary, the capability of GENs (SubG) to capture graph structural information aligns with mainstream GNN methods, and their proficiency in discerning long-range node dependencies is comparable to that of the Transformer.

Algorithm 1 computation of L -layer GENs(SubG).

Input: Graph $G = (V, E)$, node representation matrix $X^{L-1} \in \mathbb{R}^{|V| \times N}$, number of hops K , output dimension N'

Output: Node representation matrix $X^L \in \mathbb{R}^{|V| \times N'}$

- 1: Initialize weight matrices $W_1^L, W_2^L, W_q^L, W_k^L \in \mathbb{R}^{N \times N'}$ and attention vector $a \in \mathbb{R}^{2 \times N'}$; Initialize $H^{(0)} = X^{L-1}$ and $del^{(0)} = 0$;
 - 2: **for** $k = 1$ to K **do**
 - 3: $E^{(k)} \leftarrow \text{LeakyReLU}(a^T [H_i^{(k-1)} || H_j^{(k-1)}])$;
 - 4: $\alpha^{(k)} \leftarrow \text{softmax}(E^{(k)})$;
 - 5: **if** $k > 1$ **then**
 - 6: $del^{(k-1)} \leftarrow \sum_{j \in \mu(i)-i} dl^{(k-1)}$; //where $dl^{(k-1)}$ from Eq.(13)
 - 7: **end if**
 - 8: $H^{(k)} \leftarrow \sum_{j \in \mu(i)} \alpha_{ij}^{(k)} Z_j^{(k)} - del^{(k-1)}$;
 - 9: **end for**
 - 10: $\hat{H} \leftarrow \text{concat}(H^{(0)}, \dots, H^{(K)})$;
 - 11: $\beta \leftarrow H^{(0)} W_q^L (\hat{H} W_k^L)^T$;
 - 12: $X^L \leftarrow H^{(0)} W_1^L + \text{softmax}(\beta) \hat{H}_i W_2^L$;
 - 13: **return** X^L ;
-

5 EVALUATION

In this section, we conduct a comprehensive evaluation of graph elimination networks (GENs) on various graph datasets from different domains. We use the Open Graph Benchmark (OGB) to benchmark the performance of GENs on both node-level and graph-level

Table 1: The supervised learning performance across various graph-level and node-level tasks spanning multiple domains. The best results in each column are highlighted in bold, while the second-best are underscored. 'OOM' indicates that the method encountered out-of-memory issues.

Dataset	NCI1	DD	Collab	Coil-del	Cora	Arxiv	Proteins	Products	Molhiv
GCNII	81.07±1.43	77.42±2.45	79.80±1.53	74.67±1.43	81.76±1.52	72.70±0.16	76.14±0.69	72.98±0.41	77.94±1.61
DAGNN	79.22±1.43	78.10±2.56	77.93±2.52	58.41±2.92	82.53±1.65	72.09±0.25	73.26±2.14	OOM	77.46±2.03
DeeperGNN	81.09±2.13	76.49±1.24	<u>79.86±1.18</u>	62.30±2.68	81.37±1.97	71.92±0.16	OOM	OOM	<u>78.58±1.17</u>
DGMLP	80.90±1.91	76.22±2.36	77.86±1.62	66.97±2.07	82.47±1.67	72.56±0.28	<u>77.18±0.58</u>	<u>76.24±0.16</u>	78.18±1.13
GraphCON	81.07±1.28	75.46±2.12	78.82±2.67	76.89±1.92	81.69±1.89	72.12±0.23	76.84±0.48	74.57±0.11	76.43±1.12
Ordered GNN	80.21±2.13	77.33±2.97	78.98±1.55	54.95±3.00	82.73±1.63	70.93±0.23	75.50±0.52	OOM	77.80±0.51
GENs(GCN)	81.29±1.94	<u>78.67±1.42</u>	80.88±0.96	67.49±1.56	82.13±1.73	<u>72.75±0.31</u>	78.91±0.64	78.82±0.12	78.44±0.66
GENs(GAT)	80.73±1.74	78.01±2.12	79.44±0.92	65.74±2.48	81.06±2.11	72.34±0.33	OOM	OOM	77.90±1.44
GENs(SubG)	<u>81.14±1.58</u>	78.77±1.44	79.66±1.35	<u>74.76±1.45</u>	<u>82.64±1.51</u>	73.10±0.27	OOM	OOM	78.94±1.46

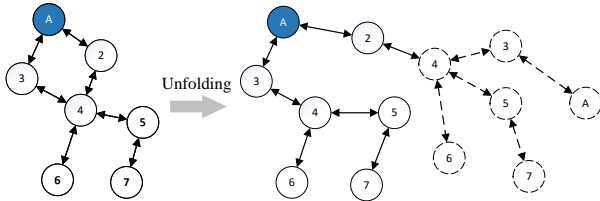


Figure 4: An illustration depicts the process of transforming a graph containing cycles into its acyclic counterpart. Nodes and edges encapsulated by the dashed boundary are projected from the original graph onto a shadow space, representing a virtual expansion of the graph. For node A, during the neighborhood aggregation phase for node representation update, the two graph representations are indiscernible up to four hops.

tasks, and supplement the graph-level tasks with the TUDataset [22]. We also perform ablation studies to investigate the effects of coupling and elimination mechanisms, as well as the choice of K , on the results under different network depths.

5.1 Experimental Settings

Datasets and Models. We use the public datasets Arxiv, Proteins, Products, and Molhiv from the OGB Large-Scale Challenge, as well as NCI1, DD, Collab, Coil-del from TUDataset and the widely used dataset Cora as our experimental datasets. All these datasets are for classification tasks, and we adopt accuracy as the evaluation metric. Table 2 summarizes the details of the datasets. We performed a comprehensive comparison between GENs and several prominent deep GNN models, namely Ordered GNN (2023)[27], GraphCON (2022)[25], DGMLP (2021)[35], DeeperGNN (2020)[18], DAGNN (2020)[21], and GCNII (2020)[5]. Within the GEN framework, we delineated three specific variants: GEN based on GCN (denoted as

Table 2: Statistics of the datasets used in the experiment.

Dataset	Graphs	Field	Avg.Nodes	Avg.Edges
NCI1	4,110	Small molecules	29.87	32.3
DD	1,178	Bioinformatics	284.32	715.66
Collab	5,000	Social networks	74.49	2457.78
Coil-del	3,900	Computer vision	21.54	54.24
Molhiv	41,127	Small molecules	25.5	27.5
Cora	1.0	Social networks	2,708	5,429
Arxiv	1.0	Social networks	169,343	1,166,243
Proteins	1.0	Bioinformatics	132,534	39,561,252
Products	1.0	Social networks	2,449,029	61,859,140

GENs(GCN)), GEN grounded in GAT (denoted as GENs(GAT)), and GENs(SubG).

Setting. We adopt different comparison criteria for the OGB datasets and the other datasets. For the OGB datasets, we follow the public leaderboard and report the mean and standard deviation of the test results that correspond to the highest validation results. For the other datasets, we use the common practice of reporting the mean and standard deviation of the highest validation results. To maintain consistency across experiments, we ensured a uniform model structure for all methods. When a model demanded identical input-output dimensionalities, linear layers were appended both at the beginning and end of the process. Otherwise, the native model structure was retained without modification. For such frameworks as GraphCON and DGMLP, GCN served as the underlying blueprint. During the parameter optimization stage, we fine-tuned model hyperparameters, including variations in layers, learning rates, and dropout settings, alongside any intrinsic parameters specific to the methods. All results are obtained from at least 10-fold cross-validation or running a single method more than 10 times. We conduct all experiments on a single NVIDIA A100 80GB GPU.

Table 3: The performance of the graph elimination networks with different K values and different numbers of layers L. K is the number of propagation steps per layer, and Res indicates the use of residual connections. GCN and GAT have the same number of layers as the product of L and K. OMM indicates that the method ran out of memory.

Arxiv	GENs (GCN) / GENs (SubG)			GCN / GAT		
	L=2	L=4	L=8 (Res)	L=2	L=4 (Res)	L=8 (Res)
K=1	70.93±0.27	72.69±0.19	72.40±0.24	71.40±0.43	72.24±0.13	72.16±0.32
K=2	72.03±0.30	72.71±0.38	72.89±0.21	-	-	71.86±0.34
K=4	72.10±0.14	72.59±0.42	72.60±0.17	-	-	71.59±0.28
K=8	71.89±0.29	72.16±0.35	71.74±0.45	-	-	70.89±0.41
K=1	70.68±0.26	72.60±0.39	72.44±0.23	71.54±0.21	72.23±0.26	72.17±0.25
K=2	71.78±0.21	72.79±0.26	72.70±0.32	-	-	71.55±0.49
K=4	72.64±0.32	73.01±0.30	OOM	-	-	OOM
K=8	71.85±0.20	OOM	OOM	-	-	OOM

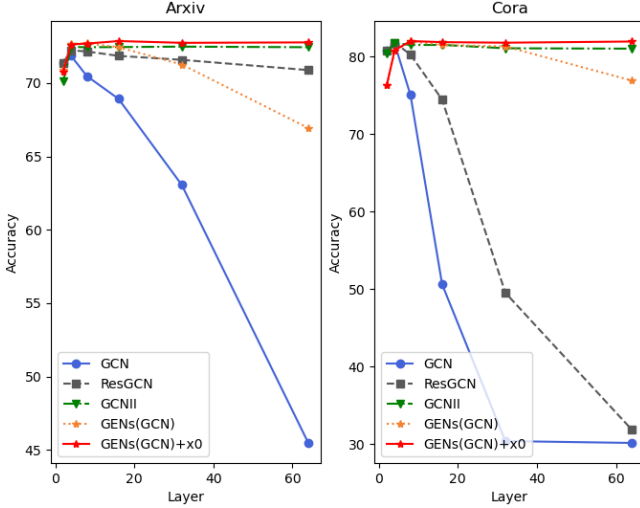


Figure 5: Illustration of the deep propagation test results. The term 'x0' indicates the addition of an initial residual connection.

In the experiments, we introduce one hyperparameter γ for GENs to balance the value decay caused by the coefficients in different hop features. Figure 3 illustrates that the multiple stacking of α leads to an imbalance between the 0th and Kth hop features on the graph. We multiply each result obtained by propagation by γ^{K-l} , where $0 < \gamma \leq 1$, $0 \leq l \leq K$, and l is the number of hops to the source node. The experimental results demonstrate that under the condition of increasing K, reducing γ appropriately can effectively improve the model performance.

5.2 Graph-Level and Node-Level Tasks

As depicted in Table 1, under the same model structure, newer methods such as Orderer GNN often show merit on specific datasets. However, when considering the overall results on graph-level and

large-scale node-level tasks, their advantage over GCNII is not as pronounced, even underperforming on certain datasets. In contrast to these approaches, our proposed GENs(GCN) and GENs(SubG) typically achieve more significant performance improvements.

Among the three methods we introduced, GENs(SubG) typically exhibits the highest performance ceiling but demands considerably more memory resources. While it cannot operate in full-batch mode for large-scale node-level data, its successful execution on the Arxiv dataset—with hundreds of thousands of nodes and millions of edges—underscores its cost-efficiency, particularly when compared to mainstream Transformer-based approaches. Additionally, the least performant of our methods is GENs(GAT), differing from GENs(SubG) only in the self-attention coefficient, beta. This stark performance disparity between them validates our theoretical analysis presented in section 4.3. Compared to the first two methods, GENs(GCN) emerges as the most cost-effective. Its performance typically lies between that of GENs(GAT) and GENs(SubG). Thanks to its support for sparse tensor computations, its computational cost is significantly lower than the other two, making it an optimal choice for balancing cost and performance.

5.3 Propagation and Ablation Studies

In this section, we evaluated the performance of GENs in deep propagation. As depicted in Figure 5, compared to GCN, the GENs(GCN) represented by the yellow line substantially decelerates the rate of performance degradation with increasing propagation steps. However, it still couldn't circumvent the node oversmoothing issue. Nonetheless, we can integrate strategies that address node oversmoothing into our model. For instance, the red line in the figure shows that after adopting an initial residual connection inspired by GCNII, the model's performance further improves and exhibits minimal decay with the increment of propagation steps.

Turning our focus to the influence of varied K values on GENs' performance across different layers of elimination networks, we employ the Arxiv dataset for this experimental segment. As Table 3 elucidates, both GCN and GAT peak at 4 layers (inclusive of the residual). In contrast, GENs (SubG) maintains a stable performance

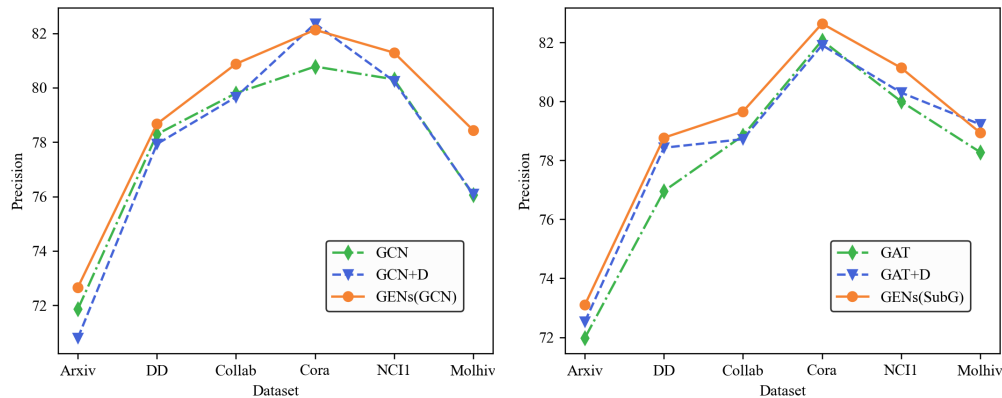


Figure 6: The results of ablation experiments on different variants of GENS. The orange line represents GENS, and the blue line represents its original network with decoupling and multiple propagation.

up to 32 hops, encompassing 8 network layers (inclusive of the residual). This highlights that while redundancy might be the primary culprit behind GNN results faltering with the addition of superficial layers, pushing the network past 32 hops still introduces performance setbacks. Further, our observations pinpoint the optimal K value range to be between 1 and 4, with minimal performance variation therein. Conclusively, optimal model performance often correlates with the number of propagation hops, with both GENS (GCN) and GENS (SubG) shining brightest at 16 hops.

To evaluate the effect of the elimination algorithm in the GENS layer, we conduct ablation experiments on different datasets in this section. We compare the performance of GENS with and without elimination, which are represented by the orange and blue lines in Figure 6, respectively. We consider two variants of GENS, namely GENS (GCN) and GENS (SubG), and their corresponding versions without elimination are denoted by GCN+D and GAT+D, respectively, where 'D' stands for decoupling. As shown in Figure 6, without elimination, simply summing up or concatenating the first and last propagation results does not usually improve the performance compared to the original GNNs, and it often performs much worse than the methods with elimination. These ablation results confirm that the elimination algorithm is essential for the graph elimination networks. However, an exception is that GAT+D surpasses our method and achieves the best result of 79.22 ± 1.25 on the OGB Molhiv dataset without elimination.

6 CONCLUSION

In this paper, we have addressed the redundancy problem in graph neural networks (GNNs), which hinders them from enlarging their receptive fields and capturing long-range dependencies. We have proposed Graph Elimination Networks (GENs), a novel model that applies graph elimination algorithms and decoupling strategies to reduce the redundancy and increase the propagation depth. We have also shown that GENs can compute the K-hop subgraph self-attention of nodes using two self-attention components, which enables them to surpass conventional GNNs in terms of expressive

power and representation learning. Our extensive experiments on various graph-level and node-level tasks have demonstrated that GENs achieve state-of-the-art results as a general network model for graph learning.

REFERENCES

- [1] Tian Bian, Xi Xiao, Tingyang Xu, Peilin Zhao, Wenbing Huang, Yu Rong, and Junzhou Huang. 2020. Rumor Detection on Social Media with Bi-Directional Graph Convolutional Networks. In *Proceedings of the AAAI Conference on Artificial Intelligence*, Vol. 34. 549–556.
- [2] Deli Chen, Yankai Lin, Wei Li, Peng Li, Jie Zhou, and Xu Sun. 2020. Measuring and Relieving the Over-Smoothing Problem for Graph Neural Networks from the Topological View. In *Proceedings of the AAAI Conference on Artificial Intelligence*, Vol. 34. 3438–3445.
- [3] Dexiong Chen, Leslie O’Bray, and Karsten Borgwardt. 2022. Structure-Aware Transformer for Graph Representation Learning. In *International Conference on Machine Learning*. PMLR, 3469–3489.
- [4] Ming Chen, Zhewei Wei, Bolin Ding, Yaliang Li, Ye Yuan, Xiaoyong Du, and Ji-Rong Wen. 2020. Scalable Graph Neural Networks via Bidirectional Propagation. *Advances in Neural Information Processing Systems* 33 (2020), 14556–14566.
- [5] Ming Chen, Zhewei Wei, Zengfeng Huang, Bolin Ding, and Yaliang Li. 2020. Simple and Deep Graph Convolutional Networks. In *International Conference on Machine Learning*. PMLR, 1725–1735.
- [6] Kien Do, Truyen Tran, and Svetha Venkatesh. 2019. Graph Transformation Policy Network for Chemical Reaction Prediction. In *Proceedings of the 25th ACM SIGKDD International Conference on Knowledge Discovery & Data Mining*. 750–760.
- [7] Wenqi Fan, Yao Ma, Qing Li, Yuan He, Eric Zhao, Jiliang Tang, and Dawei Yin. 2019. Graph Neural Networks for Social Recommendation. In *The World Wide Web Conference*. 417–426.
- [8] Wenzheng Feng, Jie Zhang, Yuxiao Dong, Yu Han, Huanbo Luan, Qian Xu, Qiang Yang, Evgeny Kharlamov, and Jie Tang. 2020. Graph Random Neural Networks for Semi-Supervised Learning on Graphs. *Advances in Neural Information Processing Systems* 33 (2020), 22092–22103.
- [9] Johannes Gasteiger, Aleksandar Bojchevski, and Stephan Günnemann. 2018. Predict then Propagate: Graph Neural Networks Meet Personalized PageRank. *arXiv preprint arXiv:1810.05997* (2018).
- [10] Justin Gilmer, Samuel S Schoenholz, Patrick F Riley, Oriol Vinyals, and George E Dahl. 2017. Neural Message Passing for Quantum Chemistry. In *International Conference on Machine Learning*. PMLR, 1263–1272.
- [11] Kai Guo, Kaixiong Zhou, Xia Hu, Yu Li, Yi Chang, and Xin Wang. 2022. Orthogonal Graph Neural Networks. In *Proceedings of the AAAI Conference on Artificial Intelligence*, Vol. 36. 3996–4004.
- [12] Will Hamilton, Zitao Ying, and Jure Leskovec. 2017. Inductive Representation Learning on Large Graphs. *Advances in Neural Information Processing Systems* 30 (2017).

- [13] Weihua Hu, Matthias Fey, Marinka Zitnik, Yuxiao Dong, Hongyu Ren, Bowen Liu, Michele Catasta, and Jure Leskovec. 2020. Open Graph Benchmark: Datasets for Machine Learning on Graphs. *Advances in Neural Information Processing Systems* 33 (2020), 22118–22133.
- [14] Wei Jin, Xiaorui Liu, Yao Ma, Charu Aggarwal, and Jiliang Tang. 2022. Feature Overcorrelation in Deep Graph Neural Networks: A New Perspective. *arXiv preprint arXiv:2206.07743* (2022).
- [15] Thomas N Kipf and Max Welling. 2016. Semi-Supervised Classification with Graph Convolutional Networks. *arXiv preprint arXiv:1609.02907* (2016).
- [16] Johannes Klicpera, Florian Becker, and Stephan Günnemann. 2021. GemNet: Universal Directional Graph Neural Networks for Molecules. *arXiv e-prints* (2021), arXiv–2106.
- [17] Guohao Li, Matthias Muller, Ali Thabet, and Bernard Ghanem. 2019. DeepGCNs: Can GCNs Go as Deep as CNNs?. In *Proceedings of the IEEE/CVF International Conference on Computer Vision*. 9267–9276.
- [18] Guohao Li, Chenxin Xiong, Ali Thabet, and Bernard Ghanem. 2020. DeeperGCN: All You Need to Train Deeper GCNs. *arXiv preprint arXiv:2006.07739* (2020).
- [19] Qimai Li, Zhichao Han, and Xiao-Ming Wu. 2018. Deeper Insights into Graph Convolutional Networks for Semi-Supervised Learning. In *Proceedings of the AAAI Conference on Artificial Intelligence*, Vol. 32.
- [20] Shuangli Li, Jingbo Zhou, Tong Xu, Dejing Dou, and Hui Xiong. 2022. GeomGCL: Geometric Graph Contrastive Learning for Molecular Property Prediction. In *Proceedings of the AAAI Conference on Artificial Intelligence*, Vol. 36. 4541–4549.
- [21] Meng Liu, Hongyang Gao, and Shuiwang Ji. 2020. Towards Deeper Graph Neural Networks. In *Proceedings of the 26th ACM SIGKDD International Conference on Knowledge Discovery & Data Mining*. 338–348.
- [22] Christopher Morris, Nils M Kriege, Franka Bause, Kristian Kersting, Petra Mutzel, and Marion Neumann. 2020. TUDataset: A Collection of Benchmark Datasets for Learning with Graphs. *arXiv preprint arXiv:2007.08663* (2020).
- [23] Kenta Oono and Taiji Suzuki. 2019. Graph Neural Networks Exponentially Lose Expressive Power for Node Classification. *arXiv preprint arXiv:1905.10947* (2019).
- [24] Yu Rong, Wenbing Huang, Tingyang Xu, and Junzhou Huang. 2019. DropEdge: Towards Deep Graph Convolutional Networks on Node Classification. *arXiv preprint arXiv:1907.10903* (2019).
- [25] T Konstantin Rusch, Ben Chamberlain, James Rowbottom, Siddhartha Mishra, and Michael Bronstein. 2022. Graph-Coupled Oscillator Networks. In *International Conference on Machine Learning*. PMLR, 18888–18909.
- [26] Alvaro Sanchez-Gonzalez, Jonathan Godwin, Tobias Pfaff, Rex Ying, Jure Leskovec, and Peter Battaglia. 2020. Learning to Simulate Complex Physics with Graph Networks. In *International Conference on Machine Learning*. PMLR, 8459–8468.
- [27] Yunchong Song, Chenghu Zhou, Xinbing Wang, and Zhouhan Lin. 2023. Ordered GNN: Ordering Message Passing to Deal with Heterophily and Over-smoothing. *arXiv preprint arXiv:2302.01524* (2023).
- [28] Indro Spinelli, Simone Scardapane, and Aurelio Uncini. 2020. Adaptive Propagation Graph Convolutional Network. *IEEE Transactions on Neural Networks and Learning Systems* 32, 10 (2020), 4755–4760.
- [29] Ashish Vaswani, Noam Shazeer, Niki Parmar, Jakob Uszkoreit, Llion Jones, Aidan N Gomez, Łukasz Kaiser, and Illia Polosukhin. 2017. Attention Is All You Need. *Advances in Neural Information Processing Systems* 30 (2017).
- [30] Petar Veličković, Guillem Cucurull, Arantxa Casanova, Adriana Romero, Pietro Lio, and Yoshua Bengio. 2017. Graph Attention Networks. *arXiv preprint arXiv:1710.10903* (2017).
- [31] Zonghan Wu, Shirui Pan, Fengwen Chen, Guodong Long, Chengqi Zhang, and S Yu Philip. 2020. A Comprehensive Survey on Graph Neural Networks. *IEEE Transactions on Neural Networks and Learning Systems* 32, 1 (2020), 4–24.
- [32] Keyulu Xu, Weihua Hu, Jure Leskovec, and Stefanie Jegelka. 2018. How Powerful are Graph Neural Networks? *arXiv preprint arXiv:1810.00826* (2018).
- [33] Ziyue Yang, Maghesree Chakraborty, and Andrew D White. 2021. Predicting Chemical Shifts with Graph Neural Networks. *Chemical Science* 12, 32 (2021), 10802–10809.
- [34] Chengxuan Ying, Tianle Cai, Shengjie Luo, Shuxin Zheng, Guolin Ke, Di He, Yanming Shen, and Tie-Yan Liu. 2021. Do Transformers Really Perform Bad for Graph Representation? *URL https://arxiv.org/abs/2106.05234* (2021).
- [35] Wentao Zhang, Zeang Sheng, Yuezhian Jiang, Yikuan Xia, Jun Gao, Zhi Yang, and Bin Cui. 2021. Evaluating Deep Graph Neural Networks. *arXiv preprint arXiv:2108.00955* (2021).
- [36] Wentao Zhang, Zeang Sheng, Ziqi Yin, Yuezhian Jiang, Yikuan Xia, Jun Gao, Zhi Yang, and Bin Cui. 2022. Model Degradation Hinders Deep Graph Neural Networks. In *Proceedings of the 28th ACM SIGKDD Conference on Knowledge Discovery and Data Mining*. 2493–2503.
- [37] Wentao Zhang, Mingyu Yang, Zeang Sheng, Yang Li, Wen Ouyang, Yangyu Tao, Zhi Yang, and Bin Cui. 2021. Node Dependent Local Smoothing for Scalable Graph Learning. *Advances in Neural Information Processing Systems* 34 (2021), 20321–20332.
- [38] Chengshuai Zhao, Shuai Liu, Feng Huang, Shichao Liu, and Wen Zhang. 2021. CSGNN: Contrastive Self-Supervised Graph Neural Network for Molecular Interaction Prediction. In *IJCAI*. 3756–3763.
- [39] Lingxiao Zhao and Leman Akoglu. 2019. PairNorm: Tackling Oversmoothing in GNNs. *arXiv preprint arXiv:1909.12223* (2019).

A APPENDIX

A.1 Derivation for Elimination Algorithm

In this section, we will give the complete derivation process of the general formula for deleting terms by the elimination algorithm using GCN as an example. First, the complete formula of GCN at the l -th layer can be described as follows:

$$h_i^{(l)} = f\left(W_l\left(C_{ii}h_i^{(l-1)} + \sum_{j \in \mu(i)-i} C_{ij}h_j^{(l-1)}\right)\right), \quad (1)$$

where $f(\cdot)$ is the nonlinear function between layers, such as the composite function Relu(BN(\cdot)) that consists of the activation function Relu and Batch Normalization. W_l is the learnable parameter matrix for the l -th layer, C_{ij} is used to normalize the node features, such that $C_{ij} = d_i^{-1/2} * d_j^{-1/2}$, and d_i denotes the degree of node i , and $h_i^{(0)} = x_i^{(0)}$, and $\mu(i)$ is the set of neighborhood nodes of node i .

Since f and W almost always occur together, we simplify the notation by omitting the parentheses between f and W in the following equations. The goal of the elimination algorithm is to eliminate the feature redundancy in the propagation process. There is no redundancy in the first layer, but since this formula will be used later, we still give it here:

$$h_i^{(1)} = fW_1\left(C_{ii}h_i^{(0)} + \sum_{j \in \mu(i)-i} C_{ij}h_j^{(0)}\right). \quad (2)$$

The second layer is calculated as follows:

$$h_i^{(2)} = fW_2\left(C_{ii}h_i^{(1)} + \sum_{j \in \mu(i)-i} C_{ij}h_j^{(1)}\right). \quad (3)$$

We try to rewrite the second term on the right side of the formula, with the goal of splitting the $h_i^{(0)}$ contained in it. At this time, there is:

$$\begin{aligned} \sum_{j \in \mu(i)-i} C_{ij}h_j^{(1)} &= \sum_{j \in \mu(i)-i} C_{ij}fW_1\left(C_{jj}h_j^{(0)}\right) \\ &\quad + C_{ji}h_i^{(0)} + \sum_{k \in \mu(j)-j-i} C_{jk}h_k^{(0)}, \end{aligned} \quad (4)$$

Given that $f(\cdot)$ is a nonlinear function, we usually cannot simplify this equation further. However, for the sake of discussion, we assume that $f(\cdot)$ is Relu = max(0, x), and that all the initial features $h^{(0)}$ have the same sign and all the parameters in the same column of W have the same sign as well. Under these assumptions, we can split the terms inside the nonlinear function. Note that C_{ij} is always non-negative, so we have:

$$\begin{aligned} \sum_{j \in \mu(i)-i} C_{ij}h_j^{(1)} &= \sum_{j \in \mu(i)-i} C_{ij}W_1 \sum_{k \in \mu(j)-j-i} C_{jk}h_k^{(0)} \\ &\quad + \sum_{j \in \mu(i)-i} C_{ij}W_1 \left| \sum_{k \in \mu(j)-j-i} C_{jk}h_k^{(0)} \right| \\ &\quad + \sum_{j \in \mu(i)-i} C_{ij}W_1 \left(C_{jj}h_j^{(0)} + C_{ji}h_i^{(0)} \right) \\ &\quad + \sum_{j \in \mu(i)-i} C_{ij} \left(W_1 \left(C_{jj}h_j^{(0)} + C_{ji}h_i^{(0)} \right) \right), \end{aligned} \quad (5)$$

there $h_i^{(1)}$ in Eq.(3) already contains features around one hop, we think that the features about 0-hop and 1-hop in the second term are redundant, that is, we need to delete the third and fourth terms

from the right side of the equation. For convenience, we denote the deleted terms as:

$$del_1 = \sum_{j \in \mu(i)-i} C_{ij}fW_1 \left(C_{jj}h_j^{(0)} + C_{ji}h_i^{(0)} \right), \quad (6)$$

so that $h_i^{(2)}$ after elimination can be written as:

$$h_i^{(2)} = fW_2\left(C_{ii}h_i^{(1)} - del_1 + \sum_{j \in \mu(i)-i} C_{ij}h_j^{(1)}\right). \quad (7)$$

In addition, according to Eq.(5), we can also get another expression of this formula:

$$h_i^{(2)} = fW_2\left(C_{ii}h_i^{(1)} + \sum_{j \in \mu(i)-i} C_{ij}fW_1 \sum_{k \in \mu(j)-j-i} C_{jk}h_k^{(0)}\right). \quad (8)$$

Continue to consider the third layer, we calculate with the same premise, first write out the formula of the third layer:

$$h_i^{(3)} = fW_3\left(C_{ii}h_i^{(2)} + \sum_{j \in \mu(i)-i} C_{ij}h_j^{(2)}\right). \quad (9)$$

According to Eq.(8), rewrite the second term in the above formula again:

$$\begin{aligned} \sum_{j \in \mu(i)-i} C_{ij}h_j^{(2)} &= \sum_{j \in \mu(i)-i} C_{ij}fW_2\left(C_{jj}h_j^{(1)}\right) \\ &\quad + \sum_{k \in \mu(j)-j} C_{jk}fW_1 \sum_{l \in \mu(k)-k-j} C_{kl}h_l^{(0)} \\ &= \sum_{j \in \mu(i)-i} C_{ij}fW_2\left(C_{jj}h_j^{(1)}\right) \\ &\quad + C_{ji}fW_1 \sum_{l \in \mu(i)-i-j} C_{il}h_l^{(0)} \\ &\quad + \sum_{k \in \mu(j)-j-i} C_{jk}fW_1 \sum_{l \in \mu(k)-k-j} C_{kl}h_l^{(0)}, \end{aligned} \quad (10)$$

since the activation function Relu guarantees that each term has the same sign, there is:

$$\begin{aligned} \sum_{j \in \mu(i)-i} C_{ij}h_j^{(2)} &= \sum_{j \in \mu(i)-i} \left(C_{ij}W_2\left(C_{jj}h_j^{(1)}\right) \right. \\ &\quad + C_{ji}fW_1 \sum_{l \in \mu(i)-i-j} C_{il}h_l^{(0)} \\ &\quad + \sum_{k \in \mu(j)-j-i} C_{jk}fW_1 \sum_{l \in \mu(k)-k-j} C_{kl}h_l^{(0)} \left. \right) \\ &\quad + C_{ij} \left(W_2\left(C_{jj}h_j^{(1)} + C_{ji}fW_1 \sum_{l \in \mu(i)-i-j} C_{il}h_l^{(0)}\right) \right) \\ &\quad + \left| W_2\left(\sum_{k \in \mu(j)-j-i} C_{jk}fW_1 \sum_{l \in \mu(k)-k-j} C_{kl}h_l^{(0)} \right) \right|. \end{aligned} \quad (11)$$

The information about two hops around the node in the above formula is unnecessary. It is important to note that the neighborhood of i necessarily contains i itself, whereas the neighborhood of j contains both i and j . However, the neighborhood of k does not have this property, and i may or may not be included in it. Therefore, we only need to delete j and k from the neighborhood of k . When k and i are connected by an edge, there is a loop in the graph, but we cannot know whether this loop exists or not. We can only assume that there is no loop here, and it is similar later. Therefore, **elimination only holds for acyclic graphs**. The deleted terms

at this time are:

$$\begin{aligned} del_2 &= \sum_{j \in \mu(i)-i} C_{ij} \left(W_2 \left(C_{jj} h_j^{(1)} + C_{ji} f W_1 \sum_{l \in \mu(i)-i-j} C_{il} h_l^{(0)} \right) \right. \\ &\quad \left. + \left| W_2 \left(C_{jj} h_j^{(1)} + C_{ji} f W_1 \sum_{l \in \mu(i)-i-j} C_{il} h_l^{(0)} \right) \right| \right) \\ &= \sum_{j \in \mu(i)-i} C_{ij} f W_2 \left(C_{jj} h_j^{(1)} + C_{ji} f W_1 \sum_{l \in \mu(i)-i-j} C_{il} h_l^{(0)} \right), \end{aligned} \quad (12)$$

where $h_l^{(0)}$ is essentially a one-hop neighborhood node of i . We transform Eq.(2) as follows:

$$h_i^{(1)} = f W_1 \left(C_{ii} h_i^{(0)} + C_{ij} h_j^{(0)} + \sum_{l \in \mu(i)-i-j} C_{il} h_l^{(0)} \right), \quad (13)$$

so, there is:

$$\begin{aligned} C_{ji} f W_1 \sum_{l \in \mu(i)-i-j} C_{il} h_l^{(0)} &= C_{ji} h_i^{(1)} \\ &\quad - C_{ji} f W_1 \left(C_{ii} h_i^{(0)} + C_{ij} h_j^{(0)} \right). \end{aligned} \quad (14)$$

Substituting Eq.(14) into Eq.(12), we have:

$$\begin{aligned} del_2 &= \sum_{j \in \mu(i)-i} C_{ij} f W_2 \left(C_{jj} h_j^{(1)} + C_{ji} h_i^{(1)} \right. \\ &\quad \left. - C_{ji} f W_1 \left(C_{ii} h_i^{(0)} + C_{ij} h_j^{(0)} \right) \right), \end{aligned} \quad (15)$$

so that $h_i^{(3)}$ after elimination can be written as:

$$h_i^{(3)} = f W_3 \left(C_{ii} h_i^{(2)} - del_2 + \sum_{j \in \mu(i)-i} C_{ij} h_j^{(2)} \right). \quad (16)$$

According to Eq.(11), $h_i^{(3)}$ can also be written as:

$$\begin{aligned} h_i^{(3)} &= f W_3 \left(C_{ii} h_i^{(2)} \right. \\ &\quad \left. + \sum_{j \in \mu(i)-i} C_{ij} f W_2 \sum_{k \in \mu(j)-j-i} C_{jk} f W_1 \sum_{l \in \mu(k)-k-j} C_{kl} h_l^{(0)} \right). \end{aligned} \quad (17)$$

Continue to consider the fourth layer, and the corresponding equation is:

$$h_i^{(4)} = f W_4 \left(C_{ii} h_i^{(3)} + \sum_{j \in \mu(i)-i} C_{ij} h_j^{(3)} \right). \quad (18)$$

Rewrite the above formula using Eq.(17). According to previous discussions, the items of f can be split directly at this point. For simplicity, we directly give the result after splitting:

$$\begin{aligned} \sum_{j \in \mu(i)-i} C_{ij} h_j^{(3)} &= \sum_{j \in \mu(i)-i} C_{ij} f W_3 \left(C_{jj} h_j^{(2)} \right. \\ &\quad \left. + \sum_{k \in \mu(j)-j} C_{jk} f W_2 \sum_{l \in \mu(k)-k-j} C_{kl} f W_1 \sum_{m \in \mu(l)-l-k} C_{lm} h_m^{(0)} \right) \\ &= \sum_{j \in \mu(i)-i} C_{ij} f W_3 \left(C_{jj} h_j^{(2)} \right. \\ &\quad \left. + C_{ji} f W_2 \sum_{l \in \mu(i)-i-j} C_{il} f W_1 \sum_{m \in \mu(l)-l-i} C_{lm} h_m^{(0)} \right) \\ &\quad + \sum_{j \in \mu(i)-i} C_{ij} f W_3 \sum_{k \in \mu(j)-j} C_{jk} f W_2 \\ &\quad \sum_{l \in \mu(k)-k-j} C_{kl} f W_1 \sum_{m \in \mu(l)-l-k} C_{lm} h_m^{(0)}. \end{aligned} \quad (19)$$

Transform Eq.(8) as follows:

$$\begin{aligned} h_i^{(2)} &= f W_2 \left(C_{ii} h_i^{(1)} + C_{ij} f W_1 \sum_{k \in \mu(j)-j-i} C_{jk} h_k^{(0)} \right. \\ &\quad \left. + \sum_{l \in \mu(i)-i-j} C_{il} f W_1 \sum_{m \in \mu(l)-l-i} C_{lm} h_m^{(0)} \right), \end{aligned} \quad (20)$$

so, there is:

$$\begin{aligned} C_{ji} f W_2 \sum_{l \in \mu(i)-i-j} C_{il} f W_1 \sum_{m \in \mu(l)-l-i} C_{lm} h_m^{(0)} &= \\ C_{ji} h_i^{(2)} - f W_2 \left(C_{ii} h_i^{(1)} + C_{ij} f W_1 \sum_{k \in \mu(j)-j-i} C_{jk} h_k^{(0)} \right). \end{aligned} \quad (21)$$

Substituting Eq.(21) into Eq.(19), we get that this layer's deleted term is:

$$\begin{aligned} del_3 &= \sum_{j \in \mu(i)-i} C_{ij} f W_3 \left(C_{jj} h_j^{(2)} + C_{ji} h_i^{(2)} \right. \\ &\quad \left. - f W_2 \left(C_{ii} h_i^{(1)} + C_{ij} f W_1 \sum_{k \in \mu(j)-j-i} C_{jk} h_k^{(0)} \right) \right). \end{aligned} \quad (22)$$

According to Eq.(2), there is such an equation:

$$h_j^{(1)} = f W_1 \left(C_{jj} h_j^{(0)} + C_{ji} h_i^{(0)} + \sum_{k \in \mu(j)-j-i} C_{jk} h_k^{(0)} \right). \quad (23)$$

The acquisition method of Eq.(23) is consistent with that of Eq.(13). The difference is only to replace node i with node j . The subscript of the final term uses j or l to indicate that there is no difference at this point. According to Eq.(23), the deleted term becomes:

$$\begin{aligned} del_3 &= \sum_{j \in \mu(i)-i} C_{ij} f W_3 \left(C_{jj} h_j^{(2)} + C_{ji} h_i^{(2)} - f W_2 \left(C_{ii} h_i^{(1)} \right. \right. \\ &\quad \left. \left. + C_{ij} h_j^{(1)} - C_{ij} f W_1 \left(C_{jj} h_j^{(0)} + C_{ji} h_i^{(0)} \right) \right) \right). \end{aligned} \quad (24)$$

so, there is:

$$h_i^{(4)} = f W_4 \left(C_{ii} h_i^{(3)} - del_3 + \sum_{j \in \mu(i)-i} C_{ij} h_j^{(3)} \right), \quad (25)$$

and there is:

$$\begin{aligned} h_i^{(4)} &= f W_4 \left(C_{ii} h_i^{(3)} + \sum_{j \in \mu(i)-i} C_{ij} f W_3 \right. \\ &\quad \left. \sum_{k \in \mu(j)-j} C_{jk} f W_2 \sum_{l \in \mu(k)-k-j} C_{kl} f W_1 \sum_{m \in \mu(l)-l-k} C_{lm} h_m^{(0)} \right). \end{aligned} \quad (26)$$

By analogy, comparing Eq.(24), Eq.(15) and Eq.(6), it can be found that any layer's deleted term del can always be simplified to a form expressed by $h_i^{(0)}$ and $h_j^{(0)}$. In order to accurately describe this deleted term, we first define a nested function as follows:

$$\begin{aligned} f_l^E &= C_{ij} f W_1 \left(C_{jj} h_j^{(0)} + C_{ji} h_i^{(0)} \right), \\ f_2^E &= C_{ij} f W_2 \left(C_{jj} h_j^{(1)} + C_{ji} h_i^{(1)} - C_{ji} f W_1 \left(C_{ii} h_i^{(0)} + C_{ij} h_j^{(0)} \right) \right), \\ &\dots \\ f_l^E &= C_{ij} f W_l \left(C_{jj} h_j^{(l-1)} + C_{ji} h_i^{(l-1)} - C_{ji} f W_{l-1} \left(C_{ii} h_i^{(l-2)} \right. \right. \\ &\quad \left. \left. + C_{ij} h_j^{(l-2)} - f W_{l-2} f_{l-2}^E \right) \right), \end{aligned} \quad (27)$$

where $l > 2$. At this time, the deleted term of layer $l + 1$ can be expressed as:

$$del_l = \sum_{j \in \mu(i)-i} f_l^E. \quad (28)$$

So that GCN eliminates computing generalization at layer $l + 1$ as follows:

$$h_i^{(l+1)} = f W_{l+1} \left(C_{ii} h_i^{(l)} - del_l + \sum_{j \in \mu(i)-i} C_{ij} h_j^{(l)} \right). \quad (29)$$

This result can be verified by experiments, as shown in Figure 1.

A.2 Algorithm Extension

In this section, we discuss how to extend the elimination algorithm to other propagation methods. For GCN propagation, C_{ij} is the same in each layer, and it is always greater than or equal to 0, but these may not hold in other propagation methods. From Eq.(4), we can see that the nonlinear function f is the main challenge for generalizing elimination. Without this function, C_{ij} and W would be unrestricted. If the nonlinear function is indispensable, then formula Eq.(5) and all subsequent formulas are only valid when C_{ij} is always positive. However, the result of Eq.(29) is not affected by the variation of C_{ij} across different layers. Assuming that C_{ij} is different in each layer, according to Eq.(27), there must be:

$$\begin{aligned} f_l^E &= C_{ij}^{(l+1)} f W_l \left(C_{jj}^{(l)} h_j^{(l-1)} + C_{ji}^{(l)} h_i^{(l-1)} \right. \\ &\quad - C_{ji}^{(l)} f W_{l-1} \left(C_{ii}^{(l-1)} h_i^{(l-2)} \right. \\ &\quad \left. \left. + C_{ij}^{(l-1)} h_j^{(l-2)} - f W_{l-2} f_{l-2}^E \right) \right). \end{aligned} \quad (30)$$

In actual code, it is not very convenient to directly calculate the above equation. We can split it as follows:

$$\begin{aligned} de_l &= C_{ji}^{(l+1)} f W_l \left(C_{ii}^{(l)} h_i^{(l-1)} + C_{ij}^{(l)} h_j^{(l-1)} - dl_{l-1} \right), \\ dl_l &= C_{ij}^{(l+1)} f W_l \left(C_{jj}^{(l)} h_j^{(l-1)} + C_{ji}^{(l)} h_i^{(l-1)} - de_{l-1} \right), \\ del_l &= \sum_{j \in \mu(i)-i} dl_l, \end{aligned} \quad (31)$$

where $de_0 = dl_0 = 0$, $C_{ij}^{(l)}$ is the propagation coefficient from node j to node i in the l -th layer, usually $C_{ij}^{(l)} \neq C_{ji}^{(l)}$. Eq.(31) is equivalent to Eq.(28), and this result applies to most mainstream GNNs. In addition, when f or W does not exist, we only need to delete f or W_l according to Eq.(31).

If we consider the simplest case, that is, assuming that C_{ij} is always 1, and f and W_3 do not exist, then Eq.(22) can be rewritten as:

$$\begin{aligned} del_3 &= \sum_{j \in \mu(i)-i} \left(h_j^{(2)} + h_i^{(2)} - \left(h_i^{(1)} + \sum_{k \in \mu(j)-j-i} h_k^{(0)} \right) \right) \\ &= \sum_{j \in \mu(i)-i} \left(h_j^{(2)} + h_i^{(2)} \right) \\ &\quad + \sum_{j \in \mu(i)-i} \left(- \left(h_i^{(1)} + \sum_{k \in \mu(j)-j-i} h_k^{(0)} \right) \right). \end{aligned} \quad (32)$$

For the first term on the right side of equation, we can rewrite it as follows:

$$\begin{aligned} \sum_{j \in \mu(i)-i} \left(h_j^{(2)} + h_i^{(2)} \right) &= (d_i - 1) h_i^{(2)} \\ &\quad + h_i^{(2)} + \sum_{j \in \mu(i)-i} h_j^{(2)}. \end{aligned} \quad (33)$$

On the one hand, according to Eq.(16), there is:

$$\sum_{j \in \mu(i)-i} \left(h_j^{(2)} + h_i^{(2)} \right) = (d_i - 1) h_i^{(2)} + h_i^{(3)} + del_2. \quad (34)$$

On the other hand, according to Eq.(12), there is:

$$del_2 = \sum_{j \in \mu(i)-i} \left(h_j^{(1)} + \sum_{l \in \mu(i)-i-j} h_l^{(0)} \right). \quad (35)$$

The second term on the right side of Eq.(32) has:

$$\sum_{j \in \mu(i)-i} \left(- \left(h_i^{(1)} + \sum_{k \in \mu(j)-j-i} h_k^{(0)} \right) \right) = -del_2. \quad (36)$$

According to Eq.(36), Eq.(34) and Eq.(32), the final Eq.(25) can be rewritten as:

$$h_i^{(4)} = (1 - d_i) h_i^{(2)} + \sum_{j \in \mu(i)-i} h_j^{(3)}. \quad (37)$$

The same result applies to Eq.(29), which means that if $C_{i,j}$ is constantly 1, and f and W do not exist, this equation can be simplified as:

$$h_i^{(l+1)} = (1 - d_i) h_i^{(l-1)} + \sum_{j \in \mu(i)-i} h_j^{(l)}, \quad (38)$$

where $l \geq 1$. When satisfying the above conditions, Eq.(38) is the simplest form to implement elimination calculation.

A.3 Simplification of the Elimination Algorithm

As we have seen in the previous section, the graph elimination algorithm can effectively eliminate feature redundancy in neighborhood aggregation, but it also has a high computational cost. Therefore, we propose a simpler and more efficient alternative: **self-loop elimination**. This method removes the self-loop from the GNN layer, which means that only nodes with odd hops or even hops in the receptive field are included in the odd or even propagation results respectively. This reduces the exponential growth of redundancy expression from per hop to every two hops, as illustrated in the lower half of Figure 1. Then, we can either sum up the outputs of all layers or just the last two layers to obtain a less redundant representation. Although self-loop elimination is not as thorough as graph elimination algorithm in removing feature redundancy, it has several advantages: it is easier to implement, more widely applicable, and often more convenient to use. However, we also note that self-loop elimination only works for acyclic graphs.

Finally, we aim to evaluate the effectiveness of self-loop elimination and graph elimination algorithms for improving the performance of graph neural networks. To this end, we conduct an experiment on different datasets and compare their performance. Figure 1 shows that graph elimination algorithm can eliminate more feature redundancy than self-loop elimination. However, our ultimate aim is to enhance the node's ability to capture the boundaries of its receptive field. In this regard, self-loop elimination and graph elimination algorithm are often equivalent, as they both remove redundant information from neighboring nodes. Moreover, self-loop elimination has a significant advantage in efficiency over graph elimination algorithm, as it avoids complex computations and supports sparse tensor operations. The only drawback of self-loop elimination is that it may interfere with the K-hop self-attention mechanism in GENs (subG). Figure 2 shows the experimental results on two variants of GENs: G1 (GCN) and G2 (SubG). The blue

Graph	Hop 1	Hop 2	Hop 3	Hop 4	Hop 5
	$\begin{bmatrix} 1 & 1 & 0 & 0 & 0 \\ 1 & 1 & 1 & 0 & 0 \\ 0 & 1 & 1 & 1 & 0 \\ 0 & 0 & 1 & 1 & 1 \\ 0 & 0 & 0 & 1 & 1 \end{bmatrix}$	$\begin{bmatrix} 1 & 1 & 1 & 0 & 0 \\ 1 & 1 & 1 & 1 & 0 \\ 1 & 1 & 1 & 1 & 1 \\ 0 & 1 & 1 & 1 & 1 \\ 0 & 0 & 1 & 1 & 1 \end{bmatrix}$	$\begin{bmatrix} 1 & 1 & 1 & 1 & 0 \\ 1 & 1 & 1 & 1 & 1 \\ 1 & 1 & 1 & 1 & 1 \\ 1 & 1 & 1 & 1 & 1 \\ 0 & 1 & 1 & 1 & 1 \end{bmatrix}$	$\begin{bmatrix} 1 & 1 & 1 & 1 & 1 \\ 1 & 1 & 1 & 1 & 1 \\ 1 & 1 & 1 & 1 & 1 \\ 1 & 1 & 1 & 1 & 1 \\ 1 & 1 & 1 & 1 & 1 \end{bmatrix}$	$\begin{bmatrix} 1 & 1 & 1 & 1 & 1 \\ 1 & 1 & 1 & 1 & 1 \\ 1 & 1 & 1 & 1 & 1 \\ 1 & 1 & 1 & 1 & 1 \\ 1 & 1 & 1 & 1 & 1 \end{bmatrix}$
	$\begin{bmatrix} 0 & 1 & 0 & 0 & 0 \\ 1 & 0 & 1 & 0 & 0 \\ 0 & 1 & 0 & 1 & 0 \\ 0 & 0 & 1 & 0 & 1 \\ 0 & 0 & 0 & 1 & 0 \end{bmatrix}$	$\begin{bmatrix} 1 & 0 & 1 & 0 & 0 \\ 0 & 2 & 0 & 1 & 0 \\ 1 & 0 & 2 & 0 & 1 \\ 0 & 1 & 0 & 2 & 0 \\ 0 & 0 & 1 & 0 & 1 \end{bmatrix}$	$\begin{bmatrix} 0 & 2 & 0 & 1 & 0 \\ 2 & 0 & 3 & 0 & 1 \\ 0 & 3 & 0 & 3 & 0 \\ 1 & 0 & 3 & 0 & 2 \\ 0 & 1 & 0 & 2 & 0 \end{bmatrix}$	$\begin{bmatrix} 2 & 0 & 3 & 0 & 1 \\ 0 & 5 & 0 & 4 & 0 \\ 3 & 0 & 6 & 0 & 3 \\ 0 & 4 & 0 & 5 & 0 \\ 1 & 0 & 3 & 0 & 2 \end{bmatrix}$	$\begin{bmatrix} 0 & 5 & 0 & 4 & 0 \\ 5 & 0 & 9 & 0 & 4 \\ 0 & 9 & 0 & 9 & 0 \\ 4 & 0 & 9 & 0 & 5 \\ 0 & 4 & 0 & 5 & 0 \end{bmatrix}$

Figure 1: The change of the node representation matrix after five times of propagation in the GCN, assume that the nodes are initially one-hot encoded, ignoring the parameters and normalization coefficients. The upper part is the result of using the graph elimination algorithm, and the lower part is the result of self-loop elimination.

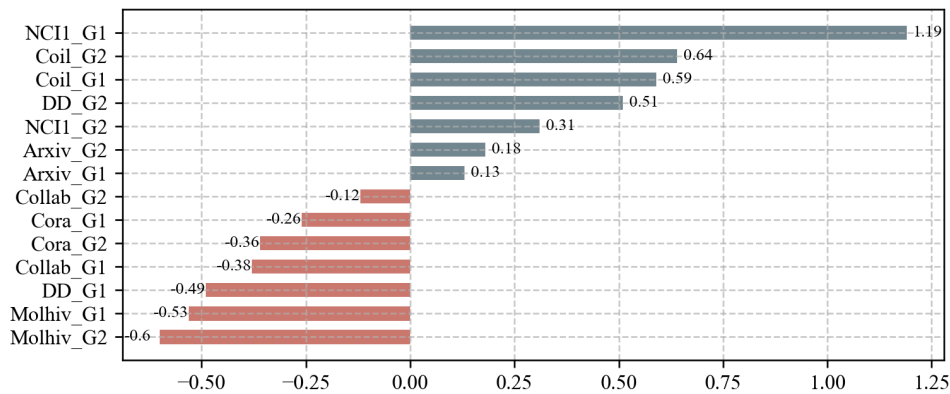


Figure 2: A comparison between self-loop elimination and applying the graph elimination algorithm on the accuracy of GENs. The values on the graph represent the difference in accuracy between the two methods, where G1 refers to GENs (GCN) and G2 refers to GENs (SubG). The blue area shows that the graph elimination algorithm outperforms self-loop elimination, while the red area shows the opposite.

part indicates that graph elimination outperforms self-loop elimination and vice versa for the red part. The results show that there

is little difference between the two elimination methods and graph elimination algorithm performs slightly better overall.